



Summertime photochemistry of the troposphere at high northern latitudes

Citation

Jacob, D. J., S. C. Wofsy, P. S. Bakwin, S.-M. Fan, R. C. Harriss, R. W. Talbot, J. D. Bradshaw, et al. 1992. "Summertime Photochemistry of the Troposphere at High Northern Latitudes." *Journal of Geophysical Research* 97, issue D15: 16421-16431.

Published Version

doi:10.1029/91JD01968

Permanent link

<http://nrs.harvard.edu/urn-3:HUL.InstRepos:14117815>

Terms of Use

This article was downloaded from Harvard University's DASH repository, and is made available under the terms and conditions applicable to Other Posted Material, as set forth at <http://nrs.harvard.edu/urn-3:HUL.InstRepos:dash.current.terms-of-use#LAA>

Share Your Story

The Harvard community has made this article openly available.
Please share how this access benefits you. [Submit a story](#).

[Accessibility](#)

Summertime Photochemistry of the Troposphere at High Northern Latitudes

D. J. JACOB,¹ S. C. WOFSY,¹ P. S. BAKWIN,¹ S.-M. FAN,¹ R. C. HARRISS,² R. W. TALBOT,²
J. D. BRADSHAW,³ S. T. SANDHOLM,³ H. B. SINGH,⁴ E. V. BROWELL,⁵ G. L. GREGORY,⁵
G. W. SACHSE,⁵ M. C. SHIPHAM,⁵ D. R. BLAKE,⁶ AND D. R. FITZJARRALD⁷

The budgets of O_3 , NO_x ($NO+NO_2$), reactive nitrogen (NO_y), and acetic acid in the 0-6 km column over western Alaska in summer are examined by photochemical modeling of aircraft and ground-based measurements from the Arctic Boundary Layer Expedition (ABLE 3A). It is found that concentrations of O_3 in the region are regulated mainly by input from the stratosphere, and losses of comparable magnitude from photochemistry and deposition. The concentrations of NO_x (10-50 ppt) are sufficiently high to slow down O_3 photochemical loss appreciably relative to a NO_x -free atmosphere; if no NO_x were present, the lifetime of O_3 in the 0-6 km column would decrease from 46 to 26 days because of faster photochemical loss. The small amounts of NO_x present in the Arctic troposphere have thus a major impact on the regional O_3 budget. Decomposition of peroxyacetyl nitrate (PAN) can account for most of the NO_x below 4-km altitude, but for only 20% at 6-km altitude. Decomposition of other organic nitrates might supply the missing source of NO_x . The lifetime of NO_y in the ABLE 3A flight region is estimated at 29 days, implying that organic nitrate precursors of NO_x could be supplied from distant sources including fossil fuel combustion at northern mid-latitudes. Biomass fire plumes sampled during ABLE 3A were only marginally enriched in O_3 ; this observation is attributed in part to low NO_x emissions in the fires, and in part to rapid conversion of NO_x to PAN promoted by low atmospheric temperatures. It appears that fires make little contribution to the regional O_3 budget. Only 30% of the acetic acid concentrations measured during ABLE 3A can be accounted for by reactions of CH_3CO_3 with HO_2 and CH_3O_2 . There remains a major unidentified source of acetic acid in the atmosphere.

1. INTRODUCTION

The Arctic Boundary Layer Expedition (ABLE 3A) surveyed the composition of the North American Arctic and sub-Arctic troposphere from the surface to 6 km altitude during July-August 1988 [Harriss *et al.*, this issue (a)]. Aircraft measurements included concentrations of O_3 , NO , NO_2 , peroxyacetyl nitrate (PAN), HNO_3 , total reactive nitrogen (NO_y), CO , non-methane hydrocarbons (NMHCs), and organic acids. We examine in this paper the photochemical activity of the regional atmosphere documented by the ABLE 3A data, with focus on the budgets of O_3 , NO_x ($NO+NO_2$), and NO_y .

Our principal objective is to explain the $\sim 1\%$ yr^{-1} rise of O_3 concentrations observed in the Arctic troposphere over the past two decades [Logan, 1985; Oltmans and Komhyr, 1986]. This rise is most pronounced in summer, averaging 3% yr^{-1} at Barrow in July for the period 1973-1984 [Oltmans and Komhyr, 1986]. Anthropogenic influence would provide a logical explanation. However, the ABLE 3A data clearly point to a stratospheric rather than to a pollution origin for O_3 in the region [Browell *et al.*, this issue; Gregory *et al.*, this issue]. This source attribution is based on three pieces of evidence: (1) concentrations of O_3 in the middle troposphere were anticorrelated with concentrations of aerosol, H_2O , and CO ; (2) well-defined layers of pollution were only marginally enriched in O_3 ; and (3) high- O_3 episodes were usually associated with stratospheric intrusions (documented by lidar). The NO_x concentrations measured in ABLE 3A were in the range 10-50 ppt [Sandholm *et al.*, this issue], sufficiently low that photochemistry should provide a net sink for O_3 . As discussed below, our analysis of the ABLE 3A data indicates that O_3 concentrations in the summertime Arctic troposphere represent largely a balance between input from the stratosphere, and losses of comparable magnitude from photochemistry and deposition.

A major point of the present paper is to show that anthropogenic influence on O_3 levels in the Arctic may manifest itself not by long-range transport of pollution-derived O_3 , but rather by a decrease of the regional photochemical sink due to the presence of small amounts of NO_x . The low concentrations of NO_x measured in ABLE 3A were sufficient to reduce the rate of photochemical loss appreciably relative to a NO_x -free atmosphere, thus increasing the O_3 lifetime. We show below that decomposition of PAN can account for most of the NO_x measured below 4-km altitude, but for only 20% at 6-km altitude. Decomposition of other organic nitrates might provide the missing source of NO_x at high altitude. Sandholm *et al.* [this issue] found that about half of total NO_y in ABLE 3A could not be accounted for by NO_x , PAN, or HNO_3 , suggesting that unidentified organic nitrates made a large contribution to the NO_y budget.

We estimate below a lifetime of 29 days for NO_y in the ABLE 3A flight region, suggesting that PAN and other organic nitrate precursors of NO_x could have been transported from distant sources. Singh *et al.* [this issue (a)] have argued that long-range transport from northern mid-latitudes was a major source of NO_y in ABLE 3A, and our analysis lends some support to that view. Concentrations of NO_y in the Arctic troposphere have therefore probably increased over the past few decades, reflecting the rise in fossil fuel combustion at northern mid-latitudes [Dignon and Hameed, 1989]. Decomposition of this anthropogenic NO_y , providing a source of NO_x in the Arctic troposphere, could then explain the observed increase of O_3 concentrations in the region.

Biomass burning emissions at high northern latitudes have also

¹ Division of Applied Sciences and Department of Earth and Planetary Sciences, Harvard University, Cambridge

² University of New Hampshire, Durham

³ Georgia Institute of Technology, Atlanta

⁴ NASA Ames Research Center, Moffett Field, California.

⁵ NASA Langley Research Center, Hampton, Virginia.

⁶ University of California, Irvine.

⁷ Atmospheric Sciences Research Center, Albany, New York.

Copyright 1992 by the American Geophysical Union.

Paper number 91JD01968.

0148-0227/92/91JD-01968\$05.00

probably increased over the past two decades, as suggested by forest fire statistics for Canada [Van Wagner, 1988; Schindler *et al.*, 1990; Stocks, 1991], but the effect on the regional O_3 budget appears to be small. The aged fire plumes sampled during ABLE 3A were only slightly enriched in O_3 [Wofsy *et al.*, this issue]. The $\Delta O_3/\Delta CO$ ratios in the plumes, where Δ represents the concentration enrichment relative to background, were in the range 0.04–0.18. In comparison, $\Delta O_3/\Delta CO$ ratios in the range 0.3–0.5 were observed in urban plumes sampled off the east coast of the United States during ABLE 3A transit flights. Andreae *et al.* [1988] previously documented $\Delta O_3/\Delta CO$ ratios in the range 0.01–0.09 for biomass fire plumes over Amazonia, as compared to 0.34 in the Manaus urban plume. Andreae *et al.* [1992] reported an average ratio of 0.14 in biomass fire plumes over the Congo. It appears that O_3 production from biomass fires, when normalized to CO emissions, is low compared to production from fossil fuel combustion. We will explain this result as due to low NO_x/CO and $NO_x/NMHC$ emission ratios in biomass fires; O_3 production is NO_x -limited, and NO_x is rapidly oxidized to organic nitrates. The relatively low NO_x emissions in biomass fires may result from low burn temperatures, particularly under smoldering conditions, and also at high latitudes from the low nitrogen content of vegetation [Chapin and Shaver, 1985].

Talbot *et al.* [this issue] measured acetic acid concentrations in the range 100–400 ppt during ABLE 3A. Acetic acid is produced by $CH_3CO_3 +$ peroxy reactions [Moortgat *et al.*, 1989a,b]. If these reactions were the dominant sources of acetic acid in the atmosphere, as has been suggested by Madronich *et al.* [1990], then acetic acid would be an interesting tracer of photochemical activity. However, we report below that only ~30% of the acetic acid measured in ABLE 3A can be accounted for in that manner. There remains a major unidentified source of acetic acid in the atmosphere.

The paper is organized in two sections. In section 2 we construct budgets of O_3 , NO_x , NO_3 , and acetic acid in the ABLE 3A flight region, using photochemical model statistics based on the aircraft observations. In section 3 we use a Lagrangian model to reconstruct the photochemical history of two aged biomass fire plumes sampled by the ABLE 3A aircraft. Concluding remarks are in section 4.

2. REGIONAL PHOTOCHEMICAL BUDGETS

Approach

We use a merged data base of chemical and meteorological measurements from ABLE 3A flights 11–25 over western Alaska (Figure 1). The data base includes 475 points in space and time for which simultaneous aircraft measurements of atmospheric composition are available. We reconstruct the local photochemical state of the atmosphere at each point, using the mechanism described in the appendix, and obtain as model products the instantaneous production and loss rates of O_3 , NO_x , PAN, HNO_3 , and acetic acid, as well as the local concentrations of short-lived species (e.g., OH). We then derive spatial and temporal averages for these products, and document the ensemble of conditions found in the regional photochemical environment.

The following measurements are used as independent variables to define the photochemical state of the atmosphere at each point: concentrations of O_3 , NO, PAN, HNO_3 , CO, ethane, propane, and butanes; and temperature, dew point, altitude, and solar zenith angle. The concentration of NO is selected as independent variable rather than the concentration of NO_x because of the sparsity of data for NO_2 . All radicals other than NO are assumed to be in

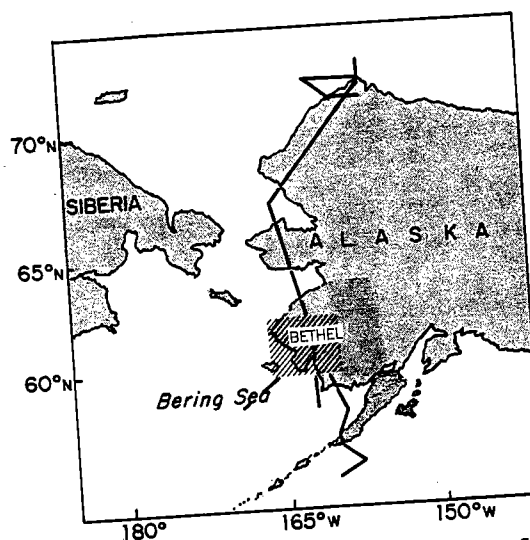


Fig. 1. ABLE 3A sampling region over western Alaska on flights 11–25 (July 19 to August 7, 1988). The dashed area around the town of Bethel was heavily sampled; additional flight tracks outside that area are shown as thick lines.

chemical steady state (including OH, peroxy species, and NO_2). Steady state is assumed also for oxygenated hydrocarbons with lifetimes of a few days or less (carbonyls, peroxides) and for other short-lived compounds (e.g., HNO_2 , HNO_4). A fixed acetone concentration of 120 ppt is adopted [Arnold *et al.*, 1986]. The UV radiation field is computed on the basis of the local altitude, solar zenith angle, and albedo, assuming clear-sky conditions (see appendix). Proper accounting of cloud effects is not possible from the data available; averaging over a large number of points should at least reduce the associated uncertainty.

The 475 points in the data base were selected on the basis of NMHC data availability. Each NMHC grab sample [Blake *et al.*, this issue] was matched with 10-s average data for O_3 , CO, and meteorological variables [Gregory *et al.*, this issue; Harriss *et al.*, this issue (b); National Aeronautics and Space Administration, 1989], 1-min average data for NO and NO_3 [Sandholm *et al.*, this issue], grab sample data for PAN [Singh *et al.*, this issue (a)], and 15 to 60 min average data for HNO_3 and acetic acid [Talbot *et al.*, this issue]. Figure 2 shows the mean vertical distributions of species concentrations in the data base. Also shown in Figure 2 are the model-calculated concentrations of OH, NO_x , and RNO_x . Here RNO_x is the residual NO_y , i.e., the fraction of observed NO_y that cannot be accounted for by measured concentrations of NO, PAN, and HNO_3 or model concentrations of NO_2 , NO_3 , N_2O_5 , HNO_2 , and HNO_4 . This residual NO_y is speculated to represent unidentified organic nitrates, hence the RNO_x notation; it accounts for about half of total NO_y .

The principal products of our analysis are the diurnally and vertically averaged photochemical rates obtained by (1) binning the individual points into 1-km altitude bands and 2-hour time intervals, (2) averaging within each bin the rates computed at individual points, and (3) averaging again over either the diurnal cycle or the 0 to 6-km column, or both. The ensemble of 475 data points covers the altitude range 0.1–6.2 km and the temporal range 0600–1915 solar time (ST); here solar time is defined by a maximum solar elevation at noon. The vertical and temporal distribution of points is shown in Figure 3. The diurnal cycle of OH concentrations in the 0 to 1-km band, where the density of points is highest, indicates a time window of active photochemistry extending from 6 to 18 ST (Figure 4).

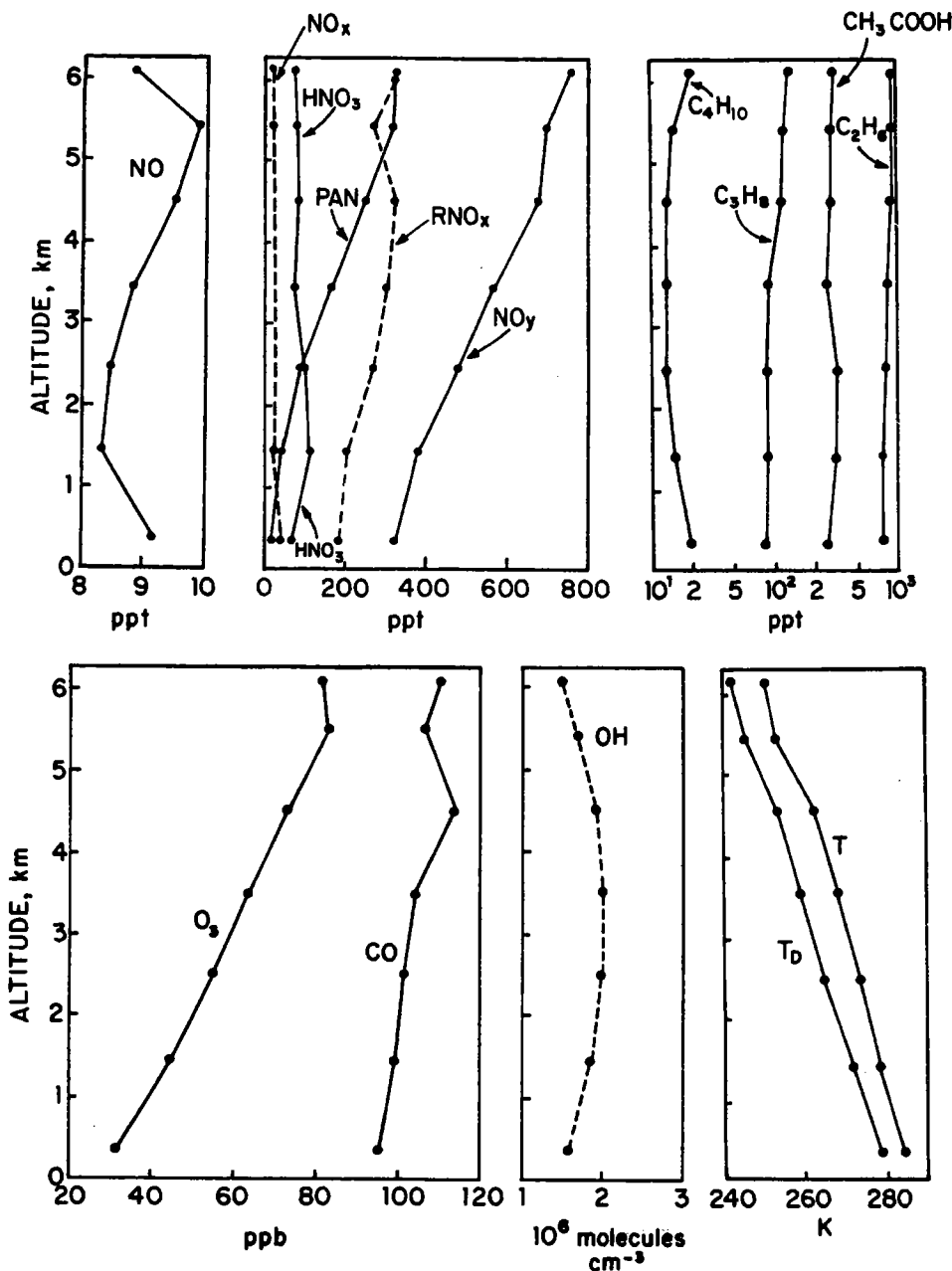


Fig. 2. Vertical distributions of species concentrations on flights 11-25 over western Alaska. The data are averages over 1-km altitude bands. Concentrations of OH, NO_x, and RNO_x (residual NO_y) are model results

and are shown as dashed lines. The OH concentration is a daytime average computed over the time window 6-18 solar time (ST). Temperature (T) and dew point (T_D) are also shown.

Inspection of Figure 3 indicates that portions of the altitude-time domain were only sparsely sampled by the aircraft. To increase the density of points, we calculate the photochemical rates for each point above 2 km altitude over a range of solar angles from 6 to 18 ST. The underlying assumption is that there should be little covariance between solar zenith angle and the other independent variables. Such an assumption would be inappropriate below 2 km because of diurnal variations driven by surface fluxes, but there is less need for increasing the density of points in that altitude range.

Ozone

Figure 5 shows the net photochemical production rate of O₃, (P-L)_{O₃}, as a function of altitude. Values are 24-hour averages computed by assuming (P-L)_{O₃} = 0 outside the 6-18 ST time win-

dow. Net O₃ loss takes place over the entire 0 to 6-km column, and is maximum between 2 and 5 km. The 24-hour average column loss rate is 8.0×10^{10} molecules cm⁻² s⁻¹, comparable in magnitude to the mean O₃ deposition flux of 8.2×10^{10} molecules cm⁻² s⁻¹ estimated by Jacob *et al.* [this issue] for the world north of 60°N in summer. Photochemistry and deposition add up to an estimated total sink of 1.6×10^{11} molecules cm⁻² s⁻¹ for O₃ in the summertime Arctic troposphere. The mean 0 to 6-km column concentration of O₃ measured during flights 11-25 was 6.4×10^{17} molecules cm⁻², from which we infer an O₃ column lifetime of 46 days. This lifetime is relatively short; we conclude that the regional O₃ budget represents largely a balance between stratospheric input on the one hand, and losses from photochemistry and deposition on the other hand.

The importance of photochemical loss as a regional sink for O₃

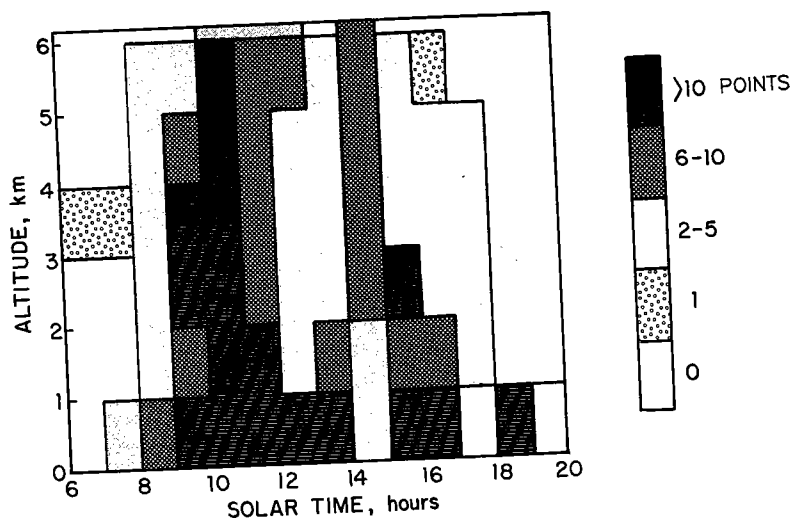
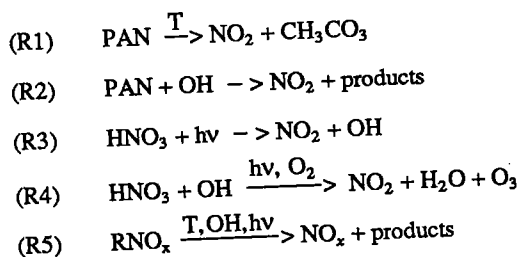


Fig. 3. Vertical and temporal distribution of the 475 points in the data base for flights 11-25.

implies that small anthropogenic perturbations to NO_x could have a major effect on O_3 levels. In the low- NO_x regime of interest here, $(\text{P-L})_{\text{O}_3}$ increases linearly with increasing NO_x concentration [Fishman *et al.*, 1979]. To assess the sensitivity of $(\text{P-L})_{\text{O}_3}$ to NO_x , we repeated our calculations for the 475 points with NO and PAN concentrations set to zero. The 24-hour average photochemical column loss rate of O_3 rose to 2.0×10^{11} molecules $\text{cm}^{-2} \text{s}^{-1}$, 2.5 times larger than in the standard calculation (Figure 5). The O_3 lifetime dropped to 26 days, 43% shorter than in the standard calculation, because of the faster photochemical loss.

Nitrogen oxides

The origin of the small amounts of NO_x measured during ABLE 3A thus emerges as a major issue in the regional O_3 budget. We expect this NO_x to represent on average a steady state between chemical sources and chemical sinks, because the lifetime against oxidation is short (~ 1 day) and emission sources are remote. The low variability of NO concentrations observed over the course of the expedition [Sandholm *et al.*, this issue] supports the argument that NO_x did not originate from direct emissions. The major chemical sources of NO_x are



and the major chemical sinks of NO_x in the daytime are

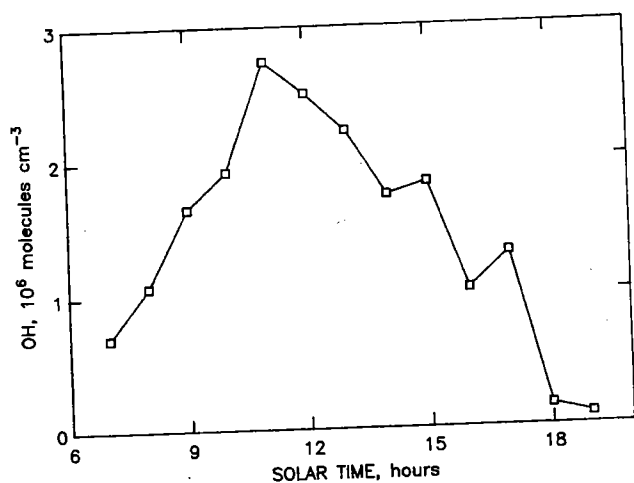
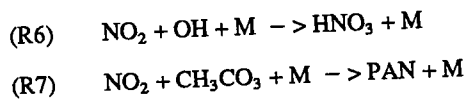


Fig. 4. Mean diurnal variation of OH concentrations below 1-km altitude on flights 11-25.

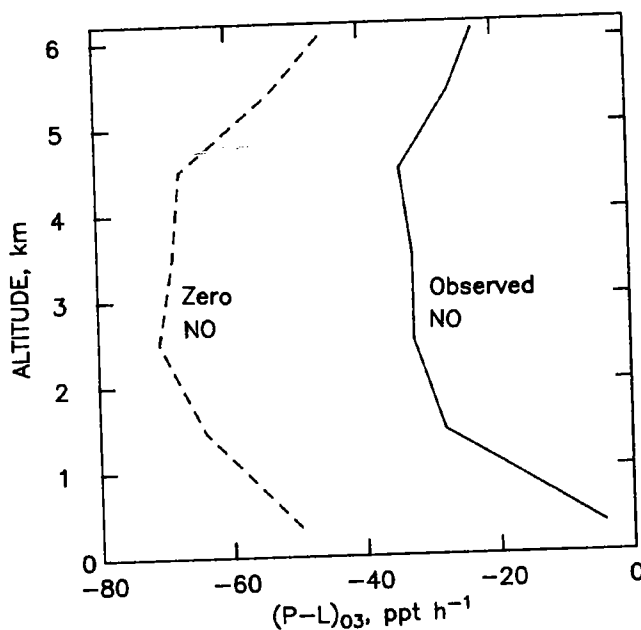
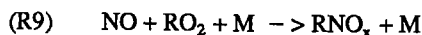
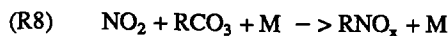


Fig. 5. Net photochemical production rates of O_3 as a function of altitude, calculated for flights 11-25 and shown as 24-hour averages for each 1-km altitude band. All values are negative, indicating net loss. The dashed line shows results from a sensitivity calculation with NO and PAN concentrations set to zero.



where RCO_3 represents peroxyacyl radicals other than CH_3CO_3 , RO_2 represents organic peroxy radicals, and RNO_x represents organic nitrates other than PAN. Reaction (R9) is a low-yield branch of the oxidation of NO by RO_2 [Lurmann et al., 1986].

Nighttime sinks of NO_x include oxidation of NMHCs by NO_3 , and hydrolysis of N_2O_5 in clouds. If these sinks were important, NO_x should be depleted at night. Although no aircraft flights were conducted during the nighttime hours, the daytime NO_x data do not indicate a depression of concentrations in the early morning, or a gradual increase of concentrations from morning to afternoon, that would be suggestive of nighttime NO_x depletion (S. T. Sandholm, personal communication, 1990). We infer that nighttime chemistry probably had only a small effect on the budget of NO_x during ABLE 3A.

For each point in the data base, we calculate the instantaneous rates of reactions (R1) through (R9) with the exception of (R5). The production of NO_x from (R5) cannot be calculated due to uncertainties on the identities, concentrations, and reactivities of the RNO_x species. We choose therefore to test the hypothesis that PAN and HNO_3 were the main sources of NO_x , i.e., that (R5) was negligible. If this hypothesis is correct, then the NO_x loss rate

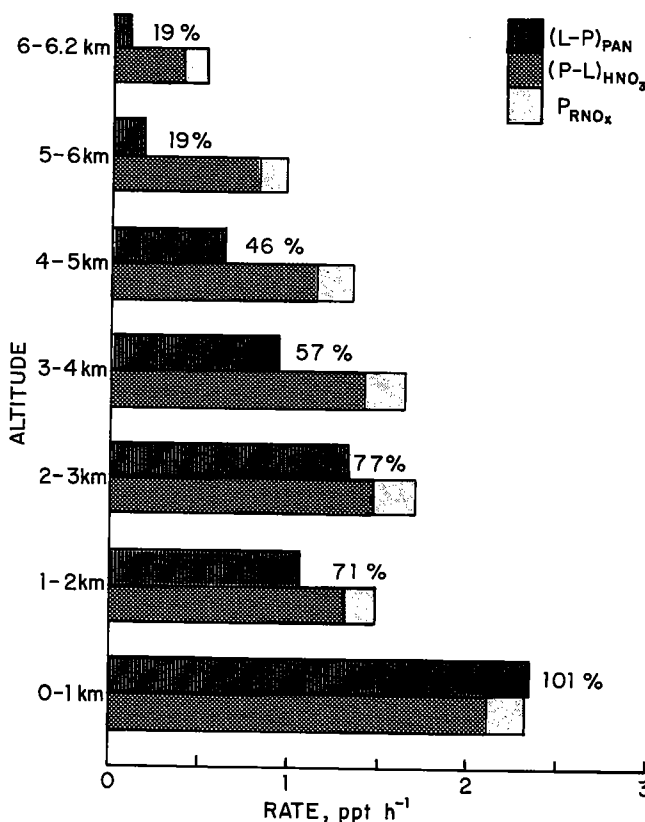


Fig. 6. Chemical production and loss rates of NO_x as a function of altitude, calculated for flights 11-25 and shown as daytime averages (6-18 ST) for each 1-km altitude band. The net production rate of NO_x from decomposition of PAN, $(L-P)_{\text{PAN}}$, is compared to the net loss rate of NO_x from oxidation to HNO_3 , $(P-L)_{\text{HNO}_3}$. The additional loss term for NO_x , P_{RNO_x} , represents production of organic nitrates other than PAN from oxidation of propane and butanes. Numbers to the right of the $(L-P)_{\text{PAN}}$ bars give the percent of the total loss rate of NO_x that is balanced by decomposition of PAN.

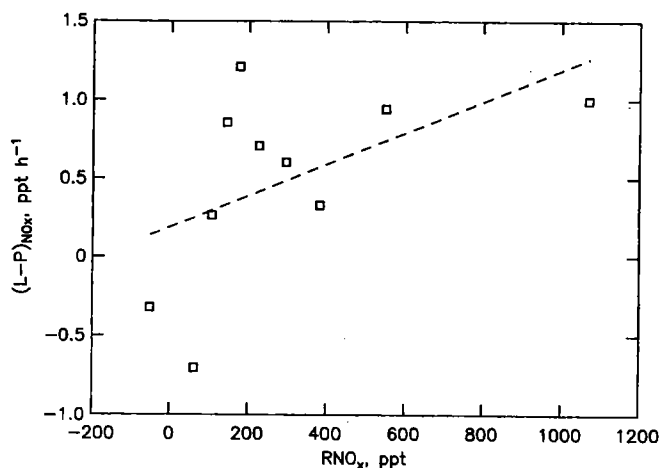


Fig. 7. Missing source of NO_x , $(L-P)_{\text{NO}_x}$, as a function of residual NO_x , (RNO_x) . The concentration of RNO_x is calculated as the difference between the concentration of NO_y and the sum of the concentrations of NO_x , NO_3 , N_2O_5 , HNO_2 , HNO_4 , PAN, and HNO_3 . Negative concentrations of RNO_x reflect uncertainties in the measurements. Results are from the 475 points in the data base for flights 11-25, ranked in order of increasing RNO_x concentration and then averaged over 50-point clusters. The dashed line is the linear regression ($r = 0.54$).

computed from $(R6)+(R7)+(R8)+(R9)$ should balance the NO_x production rate computed from $(R1)+(R2)+(R3)+(R4)$, when averaged over a large number of points and over the daytime hours (to remove transient effects from accumulation and transport terms in the NO_x budget).

Results of the analysis are shown in Figure 6, where the rates are given as averages over 1-km altitude bands and over the time window 6-18 ST. The net PAN loss rate, $(L-P)_{\text{PAN}}$, is defined as $(R1)+(R2)-(R7)$; the net HNO_3 production rate, $(P-L)_{\text{HNO}_3}$, is defined as $(R6)-(R3)-(R4)$. Also shown in Figure 6 is the production rate P_{RNO_x} of RNO_x species generated in the model by oxidation of propane and butanes. We find that net chemical loss of PAN, and net chemical production of HNO_3 , take place on average throughout the 0 to 6-km column. Below 3 km there is a close balance between production of NO_x from PAN decomposition on the one hand, and loss of NO_x by oxidation to HNO_3 and RNO_x on the other hand. At higher altitudes, however, a large fraction of the NO_x loss is not balanced by decomposition of PAN. The source of NO_x from PAN decomposition decreases rapidly with altitude because of the stability of PAN at low temperatures; the sink of NO_x from oxidation to HNO_3 decreases also with altitude but at a slower pace.

The missing source of NO_x , $(L-P)_{\text{NO}_x}$, could conceivably represent decomposition of organic nitrates other than PAN. In that case we might expect a positive correlation between $(L-P)_{\text{NO}_x}$ and the RNO_x concentration. We examined the data base for such a correlation; the analysis was done by grouping the 475 points into clusters of 50, in order of increasing RNO_x concentration, to reduce influences of local deviations of NO_x from steady state. The resulting scatter diagram indicates some positive correlation (Figure 7), although the coefficient of linear correlation is not significant at the 95% level. Changing the clustering of points did not significantly affect the result.

The atmospheric lifetime of NO_y in ABLE 3A can be estimated by assuming that deposition of HNO_3 is the only NO_y sink, and calculating the HNO_3 deposition flux needed to balance the net production rate $(P-L)_{\text{HNO}_3}$ in Figure 6. The resulting 24-hour

average HNO_3 deposition flux is 2.3×10^9 molecules $\text{cm}^{-2} \text{s}^{-1}$. The mean 0 to 6-km column concentrations of HNO_3 and NO_y measured on flights 11-25 were 8.9×10^{14} and 5.7×10^{15} molecules cm^{-2} , respectively, from which we infer HNO_3 and NO_y column lifetimes of 4.5 and 29 days, respectively.

The long lifetime of NO_y implies that distant sources could make major contributions to the NO_y budget. Singh *et al.* [this issue (a)] and Wofsy *et al.* [this issue] point to three possibly important sources of NO_y in ABLE 3A: fossil fuel combustion at mid-latitudes, biomass fires, and stratosphere-troposphere exchange. An estimate of the regional NO_y source from biomass fires can be made by using the average $\Delta\text{NO}_y/\Delta\text{CO}$ ratio of 0.0056 reported by Wofsy *et al.* [this issue] for the ABLE 3A fire plumes, and a CO emission inventory of 4×10^6 tons/month for fires north of 60°N in July (J.A. Logan, personal communication, 1992). The resulting source of NO_y is 5×10^8 molecules $\text{cm}^{-2} \text{s}^{-1}$, balancing only 20% of the NO_y sink computed above. The Logan emission inventory is based on mean fire statistics for 1975-1985, while ABLE 3A took place in 1988, but data for Canada indicate that the area burned in 1988 was about equal to the 1975-1985 average [Stocks, 1991]. It appears that biomass fires represent a significant but not dominant component of the NO_y budget at high northern latitudes.

Stratospheric input probably made a significant contribution to the NO_y budget in ABLE 3A, as indicated by the negative correlation between NO_y and CO concentrations observed in some regions of the atmosphere [Wofsy *et al.*, this issue]. However, the low HNO_3/NO_y concentration ratio at 6-km altitude (Figure 2) argues against a dominant stratospheric influence. Most of the NO_y in the lower stratosphere is present as HNO_3 [Russell *et al.*, 1988; Fahey *et al.*, 1990], and conversion of HNO_3 to organic nitrates in the upper troposphere is thought to be slow [Kasting and Singh, 1986]. It seems therefore that biomass fires and stratospheric input cannot account fully for the NO_y budget in ABLE 3A. Sources from fossil fuel combustion at northern mid-latitudes were probably important.

Acetic Acid

Our model calculations provide statistics for (1) the chemical production rate P_A of acetic acid from the reactions $\text{CH}_3\text{CO}_3 + \text{HO}_2$ and $\text{CH}_3\text{CO}_3 + \text{CH}_3\text{O}_2$, and (2) the loss rate L_A of acetic acid from reaction with OH. We still need to estimate the deposition flux of acetic acid in order to construct a regional budget. Talbot *et al.* [this issue] reported mean $\text{CH}_3\text{COOH}/\text{HNO}_3$ concentration ratios of 5 in the atmosphere and 2 in the rain, from which we infer that the lifetime of acetic acid against wet deposition was 2.5 times that of HNO_3 . The same factor may be assumed for dry deposition also [Wesely, 1989]. The lifetime of acetic acid against deposition in each 1-km altitude band is then scaled to the lifetime of HNO_3 , which is in turn calculated to balance the net production rate $(P-L)_{\text{HNO}_3}$ in that band.

Figure 8 shows the resulting acetic acid budget. Deposition and reaction with OH are sinks of comparable importance, leading to a 24-hour average total loss rate of 6.0×10^9 molecules $\text{cm}^{-2} \text{s}^{-1}$ in the 0 to 6-km column. The resulting column lifetime of acetic acid is 5.7 days, sufficiently short that concentrations should be near steady state. Figure 8 indicates, however, that production of acetic acid from $\text{CH}_3\text{CO}_3 + \text{peroxy}$ reactions can balance only 30% of the loss rate at all altitudes. Additional sources of acetic acid must therefore be important. Candidates include other permutation reactions of organic peroxy and peroxyacyl radicals [Madronech and Calvert, 1990], biogenic emissions [Keene and Galloway, 1986; Talbot *et al.*, 1990], and emissions from biomass fires [Talbot *et al.*, 1988]. A rough estimate of the regional emission

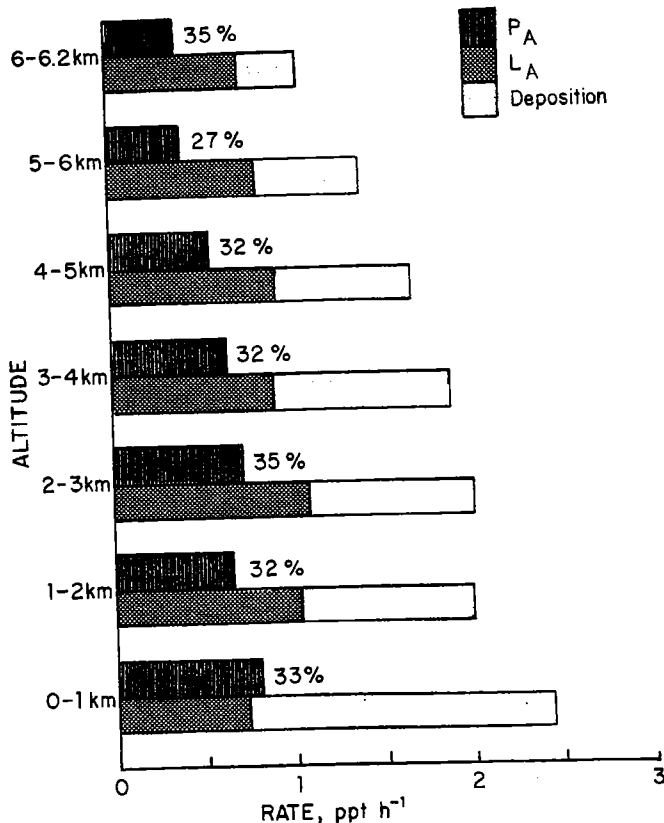


Fig. 8. Production and loss rates of acetic acid as a function of altitude, calculated for flights 11-25 and shown as 24-hour averages for each 1-km altitude band. The photochemical production rate P_A from reactions $\text{CH}_3\text{CO}_3 + \text{HO}_2$ and $\text{CH}_3\text{CO}_3 + \text{CH}_3\text{O}_2$ is compared to loss rates from reaction with OH (L_A) and deposition. Numbers to the right of the P_A bars give the percent of the total loss rate of acetic acid that is balanced by photochemical production.

from biomass fires can be made by using the enrichment ratio $\Delta\text{CH}_3\text{COOH}/\Delta\text{CO} = 0.006$ reported by Wofsy *et al.* [this issue] and the CO emission inventory cited above. We obtain an emission flux of 6×10^8 molecules $\text{cm}^{-2} \text{s}^{-1}$, balancing only 10% of the acetic acid loss rate. It would appear that emission from biomass fires is only a minor source of acetic acid on the regional scale.

3. PHOTOCHEMISTRY IN BIOMASS FIRE PLUMES

Approach

On August 3, the ABLE 3A aircraft sampled two well-defined pollution layers at 4 km altitude over the town of Bethel (Plate 1). Trajectory analyses suggest that the layers originated from thunderstorm-generated forest fires, and had traveled for 1-2 days in the middle troposphere before interception by the aircraft [Wofsy *et al.*, this issue]. The mechanism by which the fire plumes were pumped to the middle troposphere is unknown; the trajectories suggest that this pumping took place shortly after emission, possibly in the convective activity associated with the thunderstorms. The chemical composition of the pollution layers is discussed in detail by Wofsy *et al.* [this issue]. Average concentration enrichments of CO and NO_y were $\Delta\text{CO} = 80$ ppb and $\Delta\text{NO}_y = 270$ ppt. The $\Delta\text{PAN}/\Delta\text{NO}_y$ ratio was 0.23 in one layer and 0.38 in the other. No detectable enrichments of NO were observed. Enrichments of O_3 were slight, 3-6 ppb.

We reconstruct the photochemical history of these pollution layers by using a Lagrangian plume model constrained to repro-

ABLE-3A

FLIGHT 20

8-3-88

AEROSOL DISTRIBUTION

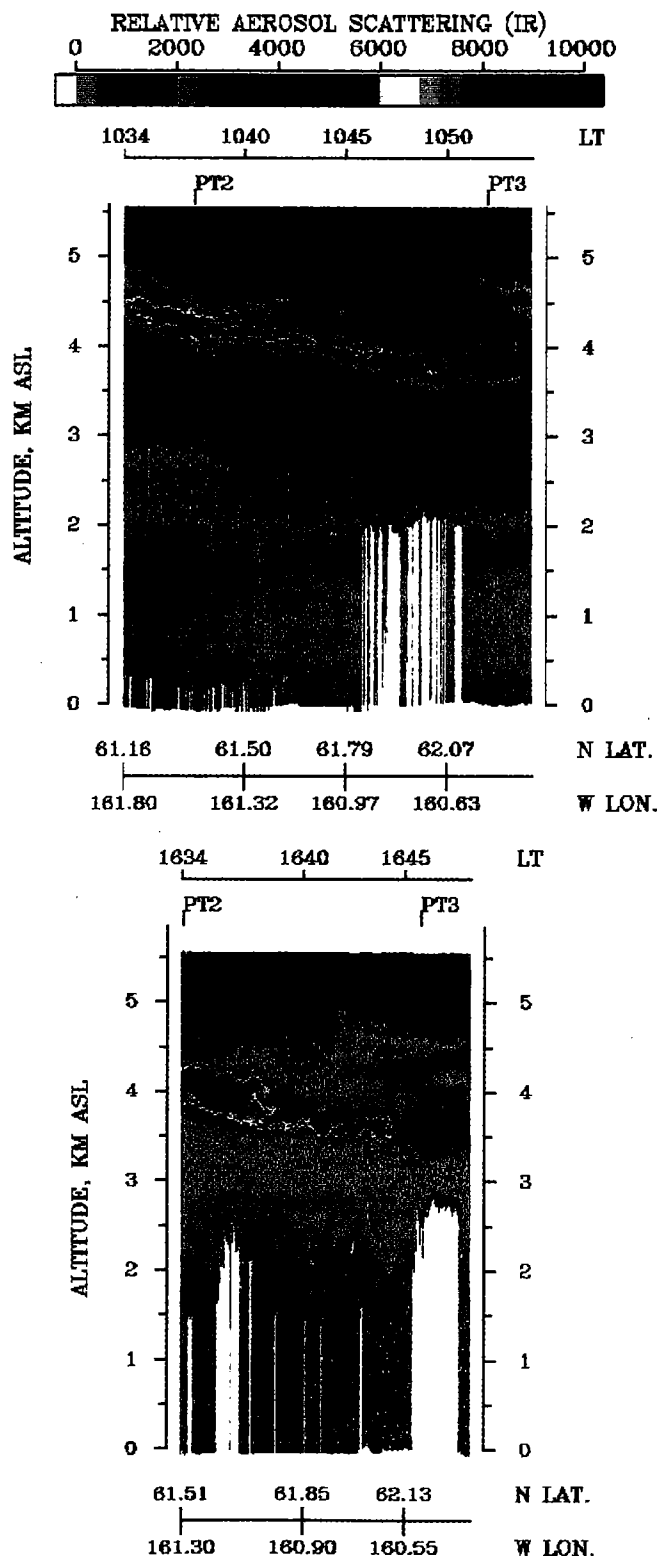


TABLE 1. Model Conditions for the Biomass Fire Plume Simulations

Species	Unit	Initial Concentration (Fresh Plume)		Background Concentration
		Diluted Plume	Diluting Plume	
CO	ppb	170	12,000	90
O ₃	ppb	50	50	50
NO _x	ppt	300	40,800	25
PAN	ppt	200	200	200
HNO ₃	ppt	50	50	50
Ethane	ppt	1400	97,000	800
Propane	ppt	500	60,000	100
Butanes	ppt	100	12,000	20
Ethylene	ppt	1200	170,000	0
Propene	ppt	370	48,000	0
Butene	ppt	90	12,000	0
Benzene	ppt	140	16,000	30
Toluene	ppt	80	7,200	30
Xylene	ppt	20	2,400	0

Background concentrations are taken from ABLE 3A observations on August 3, 1988, except for benzene and toluene concentrations, which are taken from *Rasmussen and Khalil* [1983]. The choice of initial concentrations is discussed in the text.

duce the observed enrichments ΔCO and ΔNO_y after a travel time of 2 days at 4-km altitude. Two simple schemes are used to model plume dilution: (1) instantaneous dilution upon emission, with no further dilution over the 2-day trajectory (diluted plume) and (2) horizontal dilution at a constant rate (diluting plume). These two schemes provide reasonable limiting cases; neither can pretend to capture the plume dynamics in a realistic manner, but comparison of the two gives a measure of the sensitivity of plume photochemistry to dilution rates. The width $Y(t)$ of the diluting plume at time t is computed following *Sillman et al.* [1990]:

$$Y(t) = [Y(0)^2 + 8K_y t]^{1/2} \quad (1)$$

where $Y(0)$ is the width of the fire and K_y is a constant cross-flow diffusion coefficient. Concentrations in the diluting plume are adjusted at each model time step by entrainment of background air (Table 1).

Initial conditions for the calculations (Table 1) are selected by assuming that NO_y is emitted in the fire as NO_x and that CO and NO_y are conserved over the 2-day travel time. The observed ratio $\Delta\text{NO}_y/\Delta\text{CO} = 0.0034$ [*Wofsy et al.*, this issue] then defines the NO_x/CO emission ratio. In the diluting plume case we further assume an initial CO concentration of 12 ppm and a fire width $Y(0) = 1$ km, based on data from *Cofer et al.* [1989] for a boreal forest fire in Ontario. We then adjust K_y to obtain $\Delta\text{CO} = 80$ ppb after 2 days, corresponding to a plume width of 150 km. The resulting $K_y = 1.6 \times 10^4 \text{ m}^2 \text{ s}^{-1}$ is consistent with values recommended by *Gifford* [1982] for plume widening calculations.

Initial concentrations of NMHCs are selected by assuming a NMHC/CO emission ratio of 0.10 ppbC/ppb, taken from the boreal forest fire data of *Cofer et al.* [1989]. This ratio appears typi-

Plate 1. Aerosol vertical profiles measured by downward-pointing lidar in the morning (top) and afternoon (bottom) of August 3. "LST" is local standard time (two hours ahead of solar time). Results are shown in a false color display with the relative amount of atmospheric backscattering defined by the color scale. Black represents values greater than the maximum of the color scale, i.e., strongly scattering environments (clouds, pollution layers). The black layers at 4 km altitude (top and bottom panels) are biomass fire plumes. Regions of no data, e.g., under a cloud, are shown in white.

cal of biomass fires in general, as indicated by data for selva and cerrado fires in Brazil [Greenberg *et al.*, 1984], and for a chaparral fire in California [Cofer *et al.*, 1989]. The speciation of NMHCs among alkanes, alkenes, and aromatic species is taken from Greenberg *et al.* [1984]. Initial concentrations of all secondary species (including O_3 and PAN) are assumed equal to background. Fixed temperature (268 K) and dew point (263 K) are adopted from aircraft measurements. The chemical evolution of the plume is simulated for 48 hours using the mechanism described in the appendix. The simulations are initialized at noon; initialization at midnight produced no significant differences in results.

Loss of NO_x

The NO_x concentrations in the model plumes decrease to 50 ppt during the first day of travel and drop to below background (25 ppt) by the middle of the second day (Figure 9a). The lifetime of NO_x in the fresh plumes is only 5-7 hours, consistent with the lack of a detectable ΔNO_x in the aircraft observations. The oxidation

of NO_x on the first day produces roughly equal proportions of HNO_3 and PAN, plus small amounts of other organic nitrates (Figure 9b). The high yield of PAN reflects the low $NO_x/NMHC$ emission ratio and the low temperatures. As the plumes age on the second day, slow decomposition of PAN takes place, because of the paucity of NO_x , shifting the composition of the NO_y pool towards HNO_3 and RNO_x . The $\Delta PAN/\Delta NO_x$ ratios after 2 days are 0.28 in the diluted plume and 0.38 in the diluting plume; both values fall within the range of observations.

Ozone production

Figure 9c shows the time evolution of O_3 concentrations in the model plumes. Photochemical production of O_3 is modest and confined mainly to the first day of travel when NO_x concentrations are relatively high. The decline of O_3 concentrations in the diluting plume as the plume ages is due to entrainment of background air. Simulated enrichments ΔO_3 after 2 days of travel are 4 ppb in both plumes, consistent with observations.

Photochemical production of O_3 in the model plumes is strongly NO_x -limited. Increasing NO_x emissions by a factor of 10 causes ΔO_3 to increase by a factor of 5, while increasing NMHC emissions has little effect on O_3 (Table 2). This result reflects the low $NO_x/NMHC$ emission ratio in the fire (0.034), which can be compared to typical $NO_x/NMHC$ emission ratios of 0.1-1 in U.S. cities [Environmental Protection Agency, 1989]. The NO_x/CO emission ratio in the fire (0.0034) is also low compared to typical urban values (0.05-0.1). Our finding that O_3 production in the ABLE 3A fire plumes was NO_x -limited may be applicable to biomass fire plumes in general. The review of biomass burning emissions by Crutzen and Andreae [1990] gives NO_x/CO emission ratios in the range 0.002-0.05 for various types of fires; these values are low compared to urban pollution. A likely explanation is that temperatures in biomass fires are relatively low. The particularly low NO_x/CO emission ratios in the ABLE 3A fires may reflect in addition the low nitrogen content of vegetation at high latitudes [Chapin and Shaver, 1985].

The above discussion implies that the relatively low $\Delta O_3/\Delta CO$ ratios previously reported for biomass fire plumes in the tropics [Andreae *et al.*, 1988, 1992] can be explained simply by low NO_x/CO emission ratios. The $\Delta O_3/\Delta NO_x$ ratio is an alternate measure of O_3 production in the plumes. Assuming that O_3 and NO_y are conserved in the plume, and that NO_y is emitted as NO_x , then the $\Delta O_3/\Delta NO_x$ ratio measures the number of O_3 molecules produced per molecule of NO_x emitted, i.e., the " O_3 production efficiency" [Liu *et al.*, 1987; Lin *et al.*, 1988]. The $\Delta O_3/\Delta NO_x$ ratios measured in the ABLE 3A fire plumes ranged from 12 to 21 [Wofsy *et al.*, 1991], and our model gives a value of 13 (Table 2). These values are low compared to the O_3 production efficiencies of 30-40 reported by Lin *et al.* [1988] from photochemical simulations of pollution plumes with same initial inputs of NO_x and NMHCs as in Table 1. Part of the difference appears to reflect the low temperatures in the ABLE 3A plumes, promoting conversion of NO_x to PAN.

We can estimate roughly the contribution of biomass fires plumes to the regional O_3 budget at high northern latitudes by assuming an O_3 production efficiency of 13 in the plumes, and a regional average NO_y emission flux of 5×10^8 molecules $cm^{-2} s^{-1}$ (section 2). The resulting O_3 source is 7×10^9 molecules $cm^{-2} s^{-1}$, small relative to the O_3 sink of 1.6×10^{11} molecules $cm^{-2} s^{-1}$ derived in section 2. Additional O_3 production may take place on the regional scale following dispersion of NO_y emitted from fires and eventual decomposition to NO_x . In section 2 we estimated that biomass fires could account for 20% of the NO_y budget in

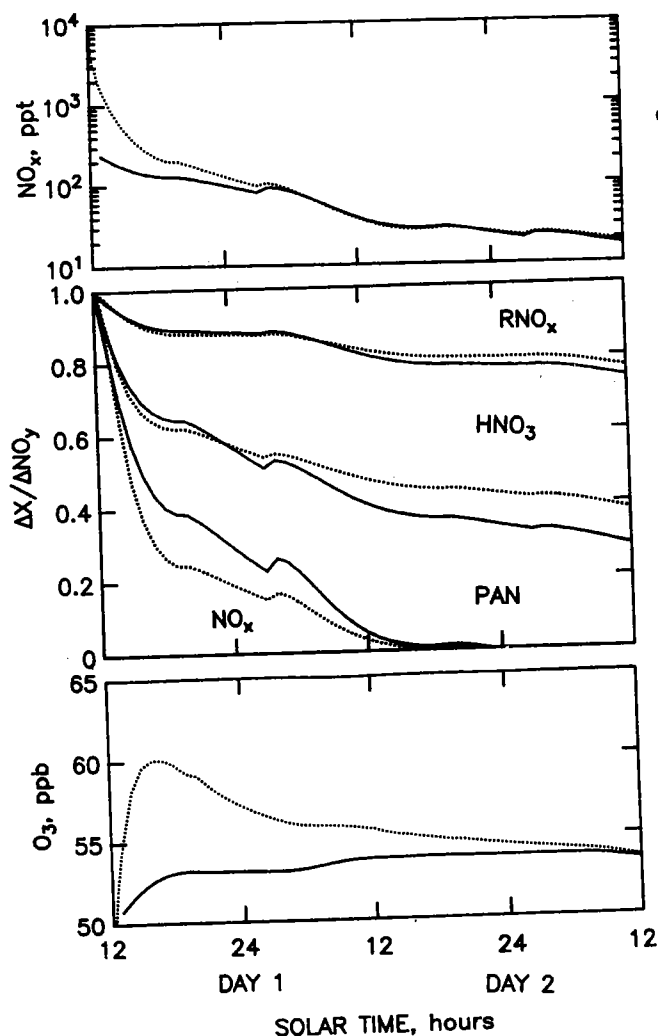


Fig. 9. Simulated chemical history of the biomass fire plumes sampled by the ABLE 3A aircraft on August 3. The calculations assume a 2-day travel time of the plumes starting at noon at the location of the fire, and ending at noon 2 days later at the location of the ABLE 3A aircraft. Results are shown for the diluted plume (solid lines) and for the diluting plume (dotted lines). (Top): Concentrations of NO_x . (Middle): Cumulative contributions of NO_x , PAN, HNO_3 , and RNO_x to ΔNO_y . (Bottom): Concentrations of O_3 .

ABLE
gional

Mo
cates
spher
spher
and d
are su
factor
atmos
pled
 NO_x
3A ha
We
 NO_x
at 6 k
be du
mosp
organ
tant
prob
Deco
sourc
 O_3 c
cades
Bi
Arcti
 O_3 i
stron
in the
repor
lowe
may
from
 O_3
3A
 CH_3
bion
acid

A
man
by J
parti
 CH_3

TABLE 2. Concentration Enrichments in the August 3 Biomass Fire Plumes

	$\Delta\text{PAN}/\Delta\text{NO}_x$ ppb/ppb	ΔO_3 ppb	$\Delta\text{O}_3/\Delta\text{NO}_x$ ppb/ppb	$\Delta\text{O}_3/\Delta\text{CO}$ ppb/ppb
Observations	0.23-0.38	3-6	12-21	0.04-0.08
Model				
1. Diluted plume	0.28	4	13	0.04
2. Diluting plume	0.38	4	13	0.04
3. NO_x emissions $\times 10$	0.12	19	7	0.24
4. NMHC emissions $\times 10$	0.41	2	8	0.03

ΔX is the concentration enrichment of species X in the plume relative to background. Observations are from *Wofsy et al.* [this issue]. Model results are shown for 2-day old plumes. The sensitivity simulations 3 and 4 were conducted with the diluted plume assumption.

ABLE 3A, suggesting that the overall influence of fires on the regional O_3 budget remains minor.

4. CONCLUSIONS

Modeling of observations from the ABLE 3A expedition indicates that the O_3 concentrations in the summertime Arctic troposphere reflect mainly a balance between input from the stratosphere, and losses of comparable magnitude from photochemistry and deposition. The observed concentrations of NO_x (10-50 ppt) are sufficiently high to reduce the O_3 photochemical loss rate by a factor of 2.5 relative to a NO_x -free atmosphere. We estimate an atmospheric lifetime of 46 days for O_3 in the 0-6 km column sampled during ABLE 3A; this lifetime would drop to 26 days if no NO_x were present. The small amounts of NO_x observed in ABLE 3A have thus a major effect on the regional O_3 budget.

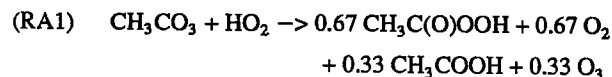
We find that decomposition of PAN can account for most of the NO_x observed in ABLE 3A below 4-km altitude, but for only 20% at 6 km altitude. The missing source of NO_x at high altitudes may be due to decomposition of unidentified organic nitrates. The atmospheric lifetime of NO_x is estimated at 29 days, implying that organic nitrate precursors of NO_x could be transported from distant sources. Long-range transport of mid-latitudes pollution probably made a substantial contribution to the NO_x budget. Decomposition of anthropogenic NO_x in the Arctic, providing a source of NO_x , could possibly explain the increase of tropospheric O_3 concentrations observed in that region over the past two decades.

Biomass fires appear to be only a minor source of O_3 in the Arctic because NO_x emissions from fires are weak. Production of O_3 in the biomass fire plumes sampled during ABLE 3A was strongly NO_x -limited. The enrichment ratios $\Delta\text{O}_3/\Delta\text{CO}$ observed in the ABLE 3A fire plumes are consistent with values previously reported for biomass fire plumes in the tropics, and are much lower than values for urban and industrial pollution. This result may be explained by the generally low NO_x/CO emission ratio from biomass burning relative to fossil fuel combustion.

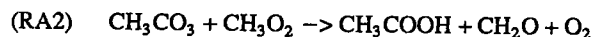
Only 30% of the acetic acid concentrations measured in ABLE 3A can be explained by reactions of CH_3CO_3 with HO_2 and CH_3O_2 . Another 10% can be explained by emissions from biomass fires. There remains a major unidentified source of acetic acid in the atmosphere.

APPENDIX: CHEMICAL MECHANISM

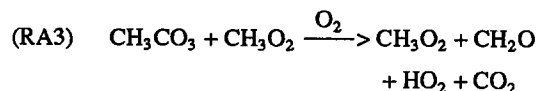
All chemical computations use the detailed mechanism of *Lurmann et al.* [1986], modified for low- NO_x conditions as described by *Jacob and Wofsy* [1988, 1990]. The modifications include in particular acetic acid production from the $\text{CH}_3\text{CO}_3 + \text{HO}_2$ and $\text{CH}_3\text{CO}_3 + \text{CH}_3\text{O}_2$ reactions [*Moortgat et al.*, 1989a,b]:



$$k = 4.3 \times 10^{-13} e^{1040/T} \text{ cm}^3 \text{ molecule}^{-1} \text{ s}^{-1}$$



$$k = 4.1 \times 10^{-15} e^{2100/T} \text{ cm}^3 \text{ molecule}^{-1} \text{ s}^{-1}$$



$$k = 1.8 \times 10^{-9} e^{-1800/T} \text{ cm}^3 \text{ molecule}^{-1} \text{ s}^{-1}$$

Loss of PAN by reaction with OH [*Wallington et al.*, 1984] is also included:



$$k = 1.2 \times 10^{-12} e^{-653/T} \text{ cm}^3 \text{ molecule}^{-1} \text{ s}^{-1}$$

Reaction with OH dominates over thermal decomposition as a sink for PAN above 5 km. Photolysis of PAN [*Senum et al.*, 1984] is negligibly slow at all altitudes of concern.

The UV radiation field is computed with a standard six-stream algorithm for the Rayleigh scattering atmosphere. The stratospheric O_3 column is 8.75×10^{18} molecules cm^{-2} (mean value for July 1988 measured at Poker Flats, Alaska). The UV albedo is 0.02 over tundra and ocean, and 0.8 over stratus decks (flight 14) and sea ice (north of 71°N). Scattering by aerosols is included with an optical depth of 0.1 at 310 nm, varying inversely with wavelength.

The calculations of section 2 solve the system of coupled algebraic equations describing the mass balances of species at steady state, with fixed input concentrations of O_3 , NO , PAN, HNO_3 , CO , methane, ethane, propane, butanes, and acetone. The time-dependent calculations of section 3 integrate the chemical mechanism over time with an implicit finite difference method.

Acknowledgments. This research was funded by the National Science Foundation (NSF-ATM-8858074 and NSF-ATM-89-21119), by the Packard Foundation, and by the Tropospheric Chemistry Program of the National Aeronautics and Space Administration. We thank J.A. Logan and R.J. Salawitch for helpful discussions and comments.

REFERENCES

- Andreae, M. O., et al., Biomass-burning emissions and associated haze layers over Amazonia, *J. Geophys. Res.*, **93**, 1509-1527, 1988.

- Andreae, M. O., A. Chapuis, B. Cros, J. Fontan, G. Helas, C. Justice, Y. J. Kaufman, A. Minga, and D. Nganga, Ozone and Aitken nuclei over equatorial Africa: airborne observations during DECAFE 88, *J. Geophys. Res.*, **97**, 6137-6148, 1992.
- Arnold, F., G. Knop, and H. Ziereis, Acetone measurements in the upper troposphere and lower stratosphere - implications for hydroxyl radical abundances, *Nature*, **321**, 505-507, 1986.
- Blake, D. R., D. F. Hurst, T. W. Smith, Jr., W. J. Whipple, T. Y. Chen, N. J. Blake, and F. S. Rowland, Summertime measurements of selected nonmethane hydrocarbons in the Arctic and sub-Arctic during the 1988 Arctic Boundary Layer Expedition (ABLE 3A), *J. Geophys. Res.*, this issue.
- Browell, E. V., F. Butler, S. A. Kooi, M. A. Fenn, R. C. Harriss, and G. L. Gregory, Large-scale variability of ozone and aerosols in summertime Arctic and sub-Arctic troposphere, *J. Geophys. Res.*, this issue.
- Chapin, F. S., III, and G. R. Shaver, Arctic, in *Physiological Ecology of North American Plant Communities*, edited by B.F. Chabot and H.A. Mooney, Chapman and Hall, New York, 1985.
- Cofer, W. R., II, J. S. Levine, D. I. Sebach, E. L. Winstead, P. J. Riggan, B. J. Stocks, J. A. Brass, V. G. Ambrosia, and P. J. Boston, Trace gas emissions from chaparral and boreal forest fires, *J. Geophys. Res.*, **94**, 2255-2259, 1989.
- Crutzen, P. J., and M. O. Andreae, Biomass burning in the tropics: Impact on atmospheric chemistry and biogeochemical cycles, *Science*, **250**, 1669-1678, 1990.
- Dignon, J. E., and S. Hameed, Global emissions of nitrogen and sulfur oxides from 1860 to 1980, *J. Air Pollut. Control Assoc.*, **39**, 180-186, 1989.
- Environmental Protection Agency, The 1985 NAPAP emission inventory (version 2): development of the annual data and modeler's tapes, *Rep. EPA/600/7-89/012a*, Research Triangle Park, N. C., 1989.
- Fahey, D. W., S. Solomon, S. R. Kawa, M. Loewenstein, J. R. Podolske, S. E. Strahan, and K.R. Chan, A diagnostic for denitrification in the winter polar stratospheres, *Nature*, **345**, 698-702, 1990.
- Fishman, J., S. Solomon, and P. J. Crutzen, Observational and theoretical evidence in support of a significant in-situ photochemical source of tropospheric ozone, *Tellus*, **31**, 432-446, 1979.
- Gifford, F. A., Horizontal diffusion in the atmosphere: a Lagrangian-dynamical theory, *Atmos. Environ.*, **16**, 505-512, 1982.
- Greenberg, J. P., P. R. Zimmerman, L. Heidt, and W. Pollock, Hydrocarbon and carbon monoxide emissions from biomass burning in Brazil, *J. Geophys. Res.*, **89**, 1350-1354, 1984.
- Gregory, G. L., B. E. Anderson, L. S. Warren, E. V. Browell, D. R. Bagwell, and C.H. Hudgins, Tropospheric ozone and aerosol observations: the Alaskan Arctic, *J. Geophys. Res.*, this issue.
- Harriss, R. C., S. C. Wofsy, D. S. Bartlett, M. C. Shipham, D. J. Jacob, J. M. Hoell, Jr., R. J. Bendura, J. W. Drewry, R. J. McNeal, R. L. Navarro, R. N. Gidge, and V. Rabine, The Arctic Boundary Layer Expedition (ABLE 3A): July-August 1988, *J. Geophys. Res.*, this issue, (a).
- Harriss, R. C., G. W. Sachse, G. F. Hill, L. Wade, K. B. Bartlett, J. E. Collins, L. R. Steele, and P. Novelli, Carbon monoxide and methane in the North American Arctic and Subarctic troposphere: July-August 1988, *J. Geophys. Res.*, this issue, (b).
- Jacob, D. J. and S. C. Wofsy, Photochemistry of biogenic emissions over the Amazon forest, *J. Geophys. Res.*, **93**, 1477-1486, 1988.
- Jacob, D. J., and S. C. Wofsy, Budgets of reactive nitrogen, hydrocarbons, and ozone over the Amazon forest during the wet season, *J. Geophys. Res.*, **95**, 16,737-16,744, 1990.
- Jacob, D. J., S.-M. Fan, S. C. Wofsy, P. A. Spiro, P. S. Bakwin, J. Ritter, E. V. Browell, G. L. Gregory, D. R. Fitzjarrald, and K. E. Moore, Deposition of ozone to tundra, *J. Geophys. Res.*, this issue.
- Kasting, J. F., and H. B. Singh, Non-methane hydrocarbons in the troposphere: Impact on odd hydrogen and odd nitrogen chemistry, *J. Geophys. Res.*, **91**, 13,239-13,256, 1986.
- Keene, W. C., and J. N. Galloway, Considerations regarding sources for formic and acetic acids in the troposphere, *J. Geophys. Res.*, **91**, 14,466-14,474, 1986.
- Lin, X., M. Trainer, and S. C. Liu, On the nonlinearity of tropospheric ozone production, *J. Geophys. Res.*, **93**, 15,879-15,888, 1988.
- Liu, S. C., M. Trainer, F. C. Fehsenfeld, D. D. Parrish, E. J. Williams, D. W. Fahey, G. Hubler, and P. C. Murphy, Ozone production in the rural troposphere and the implications for regional and global ozone distributions, *J. Geophys. Res.*, **92**, 4191-4207, 1987.
- Logan, J. A., Tropospheric ozone: Seasonal behavior, trends, and anthropogenic influence, *J. Geophys. Res.*, **90**, 10,463-10,482, 1985.
- Lurmann, F. W., A. C. Lloyd, and R. Atkinson, A chemical mechanism for use in long-range transport/acid deposition computer modeling, *J. Geophys. Res.*, **91**, 10,905-10,936, 1986.
- Madronich, S., and J. G. Calvert, Permutation reactions of organic peroxy radicals in the troposphere, *J. Geophys. Res.*, **95**, 5697-5715, 1990.
- Madronich, S., R. B. Chatfield, J. G. Calvert, G. K. Moortgaat, B. Veyret, and R. L. Lesclaux, A photochemical origin for acetic acid in the troposphere, *Geophys. Res. Lett.*, **17**, 2361-2364, 1990.
- Moortgaat, G. K., B. Veyret, and R. Lesclaux, Absorption spectrum and kinetics of reactions of the acetylperoxy radical, *J. Phys. Chem.*, **93**, 2362-2368, 1989a.
- Moortgaat, G. K., B. Veyret, and R. Lesclaux, Kinetics of the reaction of HO₂ with CH₃C(O)O₂ in the temperature range 253-368K, *Chem. Phys. Lett.*, **160**, 443-447, 1989b.
- National Aeronautics and Space Administration, GTE/ABLE 3A aircraft meteorological and navigational data, NASA Langley Research Center, Hampton, Va., 1989.
- Oltmans, S. J., and W. D. Komhyr, Surface ozone distributions and variations from 1973-1984 measurements at the NOAA Geophysical Monitoring for Climatic Change baseline observatories, *J. Geophys. Res.*, **91**, 5229-5236, 1986.
- Rasmussen, R. A., and M. A. K. Khalil, Atmospheric benzene and toluene, *Geophys. Res. Lett.*, **10**, 1096-1099, 1983.
- Russell, J. M., III, C. B. Farmer, C. P. Rinsland, R. Zander, L. Froidevaux, G. C. Toon, B. Gao, J. Shaw, and M. Gunson, Measurements of odd nitrogen compounds in the stratosphere by the ATMOS experiment on Spacelab 3, *J. Geophys. Res.*, **93**, 1718-1736, 1988.
- Sandholm, S.T., et al., Tropospheric observations related to N₂O_y distributions and partitioning over the Alaskan Arctic, *Journal of Geophysical Research*, this issue.
- Schindler, D. W., K. G. Beaty, E. J. Fee, D. R. Cruikshank, E. R. DeBruyn, D. L. Findlay, G. A. Linsey, J. A. Shearer, M. P. Stainton, and M. A. Turner, Effects of climatic warming on lakes of the central boreal forest, *Science*, **250**, 967-970, 1990.
- Senum, G. I., Y.-N. Lee, and J. S. Gaffney, Ultraviolet absorption spectrum of peroxyacetyl nitrate and peroxypropionyl nitrate, *J. Phys. Chem.*, **88**, 1269-1270, 1984.
- Sillman, S., J. A. Logan, and S. C. Wofsy, A regional scale model for ozone in the United States with subgrid representation of urban and power plant plumes, *J. Geophys. Res.*, **95**, 5731-5748, 1990.
- Singh, H. B., D. O'Hara, D. Herlth, J. D. Bradshaw, S. T. Sandholm, G. L. Gregory, G. W. Sachse, D. R. Blake, P. J. Crutzen, and M. A. Kanakidou, Atmospheric measurements of peroxyacetyl nitrate and other organic nitrates at high latitudes: Possible sources and sinks, *J. Geophys. Res.*, this issue, (a).
- Singh, H. B., D. Herlth, D. O'Hara, K. Zahnle, J. D. Bradshaw, S. T. Sandholm, R. Talbot, P. J. Crutzen, and M. Kanakidou, Relationship of peroxyacetyl nitrate to active and total odd nitrogen at northern high latitudes: Influence of reservoir species on NO_x and O₃, *J. Geophys. Res.*, this issue, (b).
- Stocks, B. J., The extent and impact of forest fires in northern circumpolar countries, in *Global Biomass Burning*, edited by J. Levine, 197-202, MIT Press, Cambridge, Mass., 1991.
- Talbot, R. W., K. M. Beecher, R. C. Harriss, and W. R. Cofer III, Atmospheric geochemistry of formic and acetic acids at a mid-latitude temperate site, *J. Geophys. Res.*, **93**, 1638-1652, 1988.
- Talbot, R. W., M. O. Andreae, H. Berresheim, D. J. Jacob, and K. M. Beecher, Sources and sinks of formic, acetic, and pyruvic acids over cen-

- tral Amazonia, 2, Wet season, *J. Geophys. Res.*, **95**, 16,799-16,812, 1990.
- Talbot, R. W., A. S. Vijgen, and R. C. Harriss, Soluble species in the Arctic summer troposphere: Acidic gases, aerosols, and precipitation, *J. Geophys. Res.*, this issue.
- Van Wagner, C. E., The historical pattern of annual burned area in Canada, *The Forestry Chronicle*, pp. 182-185, June 1988.
- Wallington, T. J., R. Atkinson, and A. M. Winer, Rate constants for the gas phase reaction of OH radicals with peroxyacetyl nitrate (PAN) at 273 and 297 K, *Geophys. Res. Lett.*, **11**, 861-864, 1984.
- Wesely, M. L., Parameterization of surface resistance to gaseous dry deposition in regional-scale numerical models, *Atmos. Environ.*, **23**, 1293-1304, 1989.
- Wofsy, S. C., et al., Atmospheric chemistry in the Arctic and sub-Arctic: Influence of natural fires, industrial emissions, and stratospheric inputs, *J. Geophys. Res.*, this issue.
- P. S. Bakwin, S.-M. Fan, D. J. Jacob, and S. C. Wofsy, Division of Applied Sciences and Department of Earth and Planetary Sciences, Harvard University, Cambridge, MA 02138.
- D. R. Blake, University of California, Irvine, CA 92714.
- J. D. Bradshaw and S. T. Sandholm, Georgia Institute of Technology, Atlanta, GA 30332.
- E. V. Browell, G. L. Gregory, G. W. Sachse, and M. Shipman, NASA Langley Research Center, Hampton, VA 23665.
- D. R. Fitzjarrald, Atmospheric Sciences Research Center, Albany, NY 12205.
- R. C. Harriss and R. W. Talbot, University of New Hampshire, Durham, NH 03824.
- H. B. Singh, NASA Ames Research Center, Moffett Field, CA 94035.

(Received November 30, 1990;
revised July 26, 1991;
accepted July 26, 1991.)